9-7-2016

Recent trends in vegetation greenness in China significantly altered annual evapotranspiration and water yield

Yibo Liu
Nanjing University of Information Science and Technology

Jingfeng Xiao
University of New Hampshire, Durham, j.xiao@unh.edu

Weimin Ju
Nanjing University

Ke Xu
University of Wisconsin Madison

Yanlian Zhou
Nanjing University

See next page for additional authors

Authors
Yibo Liu, Jingfeng Xiao, Weimin Ju, Ke Xu, Yanlian Zhou, and Yantai Zhao

Recent trends in vegetation greenness in China significantly altered annual evapotranspiration and water yield

2016 Environ. Res. Lett. 11 094010

(http://iopscience.iop.org/1748-9326/11/9/094010)

Environmental Research Letters

LETTER

Recent trends in vegetation greenness in China significantly altered annual evapotranspiration and water yield

Yibo Liu[1,2], **Jingfeng Xiao**[2,3], **Weimin Ju**[4], **Ke Xu**[5], **Yanlian Zhou**[6] **and Yuntai Zhao**[7]

[1] Jiangsu Key Laboratory of Agricultural Meteorology, School of Applied Meteorology, Nanjing University of Information Science and Technology, Nanjing, 210044, People's Republic of China
[2] Earth Systems Research Center, Institute for the Study of Earth, Oceans, and Space, University of New Hampshire, Durham, NH 03824, USA
[3] International Center for Ecology, Meteorology, and Environment, School of Applied Meteorology, Nanjing University of Information Science and Technology, Nanjing, 210044, People's Republic of China
[4] International Institute for Earth System Sciences, Nanjing University, Nanjing, 210023, People's Republic of China
[5] Department of Atmospheric and Oceanic Sciences & Center for Climate Research, University of Wisconsin Madison, Madison, WI 53706, USA
[6] School of Geographic and Oceanographic Sciences, Nanjing University, Nanjing, 210023, People's Republic of China
[7] China Land Surveying and Planning Institute, Beijing, 10035, People's Republic of China

E-mail: j.xiao@unh.edu

Keywords: vegetation greenness, greening, browning, water yield, evapotranspiration, afforestation, leaf area index

Supplementary material for this article is available online

OPEN ACCESS

RECEIVED
5 April 2016

REVISED
20 July 2016

ACCEPTED FOR PUBLICATION
15 August 2016

PUBLISHED
7 September 2016

Abstract

There has been growing evidence that vegetation greenness has been increasing in many parts of the northern middle and high latitudes including China during the last three to four decades. However, the effects of increasing vegetation greenness particularly afforestation on the hydrological cycle have been controversial. We used a process-based ecosystem model and a satellite-derived leaf area index (LAI) dataset to examine how the changes in vegetation greenness affected annual evapotranspiration (ET) and water yield for China over the period from 2000 to 2014. Significant trends in vegetation greenness were observed in 26.1% of China's land area. We used two model simulations driven with original and detrended LAI, respectively, to assess the effects of vegetation 'greening' and 'browning' on terrestrial ET and water yield. On a per-pixel basis, vegetation greening increased annual ET and decreased water yield, while vegetation browning reduced ET and increased water yield. At the large river basin and national scales, the greening trends also had positive effects on annual ET and had negative effects on water yield. Our results showed that the effects of the changes in vegetation greenness on the hydrological cycle varied with spatial scale. Afforestation efforts perhaps should focus on southern China with larger water supply given the water crisis in northern China and the negative effects of vegetation greening on water yield. Future studies on the effects of the greenness changes on the hydrological cycle are needed to account for the feedbacks to the climate.

1. Introduction

There has been growing evidence that vegetation greenness has been increasing in many parts of the northern middle and high latitudes during the last three to four decades (Xiao and Moody 2005, de Jong *et al* 2011, Zhou *et al* 2011, Guay *et al* 2014). The evidence is mainly from the satellite-derived normalized difference vegetation index (NDVI) or leaf area index (LAI). The 'greening' of the land surface can be attributed to various factors such as plant growth, afforestation/reforestation, and improved agricultural practices. Changes in vegetation greenness can alter the water balance by regulating matter and energy cycles (Bonan 2008).

Changes in vegetation cover or productivity influence the hydrological cycle mainly through modulating the processes of canopy interception, evaporation and transpiration (referred to as evapotranspiration or ET hereafter), and infiltration. The relationship

between vegetation cover particularly forest cover and water yield remains hotly contested (Ellison *et al* 2012). Some studies showed that afforestation or reforestation could reduce available water supply (Zhang *et al* 2001, Andréassian 2004, Brown *et al* 2005, Jackson *et al* 2005). Increasing tree cover increases canopy interception and ET and thereby reduces run-off, leading to declining water availability. These studies are largely based on small-scale studies including paired-catchment experiments in small catchments. By contrast, some other studies showed that increasing forest cover can facilitate large-scale transport of water vapor and promote precipitation at regional to global scales, and therefore forest cover may have positive impacts on the hydrological cycle (Makarieva *et al* 2006, Liu *et al* 2008b, Sheil and Murdiyarso 2009, Jiang and Liang 2013, Zhang *et al* 2015a). Despite the large number of studies, the effects of vegetation greening particularly afforestation on the hydrological cycle have been controversial.

Trends of vegetation greening have been observed in many areas of China (Xiao and Moody 2004, Park and Sohn 2010, Li *et al* 2012, Chen *et al* 2014, Xiao 2014). China has the largest area of forest plantations in the world. Afforestation and reforestation have been nationwide efforts in China since the 1950s. To mitigate environmental degradation, the Chinese government also implemented multiple large-scale ecosystem restoration programs, including the 'Three-North Forest Shelterbelt Program', and the 'Natural Forest Conservation Program', and the 'Grain for Green Program'. These efforts substantially increased the national forest area (Gao *et al* 2014, Chen *et al* 2015, Zhang *et al* 2015b). Improved agricultural practices including the use of irrigation and chemical fertilizers and the substitution of high-yield crops for low-yield corps led to the increase of agricultural productivity (Xiao and Moody 2004, Xiao *et al* 2015). Global change factors including climatic warming, rising atmospheric carbon dioxide (CO_2) concentrations, and nitrogen deposition enhanced plant growth (Tian *et al* 2011, Xiao *et al* 2015). In the meanwhile, natural vegetation decreased because of ecosystem degradation and rapid urbanization (Wang *et al* 2012, Liu *et al* 2012a), leading to decreases in vegetation cover or productivity ('browning') in some parts of the country. The changes in vegetation greenness could alter the regional carbon and water cycles and the local surface climate.

Several studies showed that increasing vegetation cover resulting from afforestation and ecosystem restoration in China reduced streamflow (Huang *et al* 2003, Bao *et al* 2012, Li *et al* 2014, Liu *et al* 2015a). For example, the simulations of a hydrological model indicated that forestation may reduce average water yield by 50% in the semi-arid Loess Plateau region in northern China and 30% in the tropical southern region (Sun *et al* 2006). By contrast, Xie *et al* (2015) indicated that afforestation practices had negligible effects on the hydrological cycle over the Three-North region of China. Moreover, the results based on an ecosystem model indicated that deforestation across China increased ET and decreased water yield while reforestation dcecreased ET (Liu *et al* 2008a). Previous studies therefore are inconsistent regarding the effects of afforestation/reforestation on the hydrological cycle. A recent study showed that the increase in urban areas and the reduction of rice paddy fields reduced ET by 23% and increased streamflow by 58% in the Qinhuai River basin in southern China (Hao *et al* 2015b). Better understanding how the changes in vegetation greenness affect ET and water yield has ecohydrological implications and can inform regional and national afforestation/reforestation policies.

In this study, we used a process-based ecosystem model and a satellite-derived LAI dataset to examine the effects of vegetation greening and browning on annual ET and water yield for China over the period from 2000 to 2014. First, the LAI dataset was used to assess the linear trends of vegetation greenness. Second, the 'greening' or 'browning' trend was removed on a per-pixel basis by detrending LAI. Third, we used a process-based ecosystem model—Boreal ecosystem production simulator (BEPS) along with the original and detrended LAI datasets to conduct two model simulations: one with original LAI (i.e., with trends of vegetation greening and browning) and one with detrended LAI (i.e., with no trends of vegetation greening or browning). Finally, the two model simulations were used to assess the effects of vegetation greening and browning on terrestrial ET and water yield.

2. Data and methods

2.1. Model description

We used the process-based ecosystem model—BEPS (Liu *et al* 1997) to assess how the trends in vegetation greenness affect annual ET and water yield in China. The BEPS model is run at half-hourly to daily time step, and is driven by meteorological variables (temperature, precipitation, incoming solar radiation, and relative humidity), remotely sensed LAI, land cover type, atmospheric CO_2 concentrations, and soil properties data. The BEPS model consists of hydrology, photosynthesis, energy balance, and soil biogeochemistry modules (Ju *et al* 2010b). This model stratifies a canopy into sunlit and shaded leaves, for which daily carbon fixation and transpiration are separately calculated (Chen *et al* 1999). ET of an ecosystem is calculated as the sum of canopy transpiration from sunlit and shaded leaves, and evaporation from soil surface and intercepted water by leaf surface. Both transpiration and evaporation are calculated using the Penman–Monteith equation (Chen *et al* 2005). The BEPS model has been continuously improved and has been applied to simulate hydrological processes for a wide variety of terrestrial ecosystems (Ju *et al* 2010a,

Zhang *et al* 2013, Liu *et al* 2013b, 2015b). More details about this model can be found elsewhere (Liu *et al* 1997, 2003, 2013b, Chen *et al* 1999, 2005, Ju *et al* 2006).

2.2. Driving datasets

In this study, vegetation greenness in China was characterized using a gridded LAI dataset derived from the moderate resolution imaging spectroradiometer (MODIS) (Liu *et al* 2015b). This LAI dataset consists of 8 day LAI composites with 500 m spatial resolution from 2000 to 2014. The LAI data were retrieved from the 8 day MODIS reflectance product (MOD09A1 V05) (Vermote and Vermeulen 1999) and the yearly MODIS land cover datasets (MCD12Q1 V051) (Friedl *et al* 2010) using a 4-scale geometric optical model (Deng *et al* 2006, Liu *et al* 2012b). Previous studies indicated that the 4-scale geometric optical model was superior to the algorithm used to produce the MODIS LAI product (Pisek *et al* 2007, Garrigues *et al* 2008). We used the 500 m resolution LAI dataset to examine the trends of vegetation greenness and to prescribe LAI for the BEPS model simulations.

We used gridded daily precipitation, maximum and minimum air temperatures, incoming solar radiation, and relative humidity from a gridded meteorological dataset with 500 m spatial resolution. This dataset was interpolated from observations from 753 weather stations across China using the inverse distance weight method (Liu *et al* 2015b). The accuracy of the daily gridded meteorological dataset was evaluated at the site level using daily temperature, precipitation, and radiation measurements from 8 eddy covariance (EC) flux sites (http://chinaflux.org). The comparison showed that the daily radiation and temperature exhibited excellent agreement between the gridded dataset and the tower observations with R^2 values ranging from 0.77 to 0.92 for daily radiation and 0.90 to 0.99 for daily temperature, respectively (figures S1 and S2). The consistence was lower for daily precipitation (figure S3) because of the complexity of precipitation dynamics and the missing data of the EC sites. We also evaluated the gridded meteorological dataset using monthly 0.5° precipitation and temperature data in 2000 obtained from China Meteorological Administration (http://cdc.cma.gov.cn). Both annual precipitation and annual mean temperature showed high consistency between the two datasets (figure S4).

Soil data used here include volumetric fractions of clay, sand, and silt data. This soil dataset was developed based on 8595 soil profile records compiled from the second national soil survey dataset and the 1: 1000 000 scale soil map of China (Shangguan *et al* 2012).

Atmospheric CO_2 concentration values were based on the annual mean CO_2 measurements at Mauna Loa Observatory, Hawaii (Keeling *et al* 1976). The CO_2 time series was obtained from the National Oceanic and Atmospheric Administration's Earth System Research Laboratory (http://esrl.noaa.gov/gmd/ccgg/trends/).

2.3. Trends and detrending analyses of LAI

We assessed the trends of vegetation greenness for the period 2000–2014 using the gridded LAI dataset. For each pixel, we calculated the annual mean LAI for each year by averaging the 8 day LAI values throughout the year. We then examined the linear trend of annual LAI over the 15 year period by regressing LAI as a function of time on a per-pixel basis. The following linear regression model was used to quantify the linear trend of annual mean LAI:

$$y = a + bt, \tag{1}$$

where y is LAI, t is time (year), and a and b are the intercept and slope, respectively. The significance level (α) of 0.05 was used for the trend analysis. Increasing LAI indicates a greening trend, while decreasing LAI indicates a browning trend.

To quantitatively assess the effects of greening and browning on annual ET and water yield, we detrended the LAI time series on a per-pixel basis, following previous studies (Wang and You 2004, Xiao *et al* 2015). For each pixel, we determined the linear fit between annual mean LAI and time and then removed the linear fit from the variable:

$$y_r = y - \hat{y}, \tag{2}$$

where y_r is the detrended LAI, y is the original LAI, and $\hat{y}$ is the fitted LAI derived from equation (1). The detrended time series—y_r is essentially the residuals from the linear fit. For each pixel, we then generated the new LAI time series:

$$y_n = y_{2000} + y_r, \tag{3}$$

where y_n is the new annual mean LAI time series, and y_{2000} is the annual mean LAI value in 2000. The new annual mean LAI time series (y_n) maintains the interannual variations but has no linear trends. The residuals y_r of each year were assigned to every 8 day composite based on the proportion the 8 day LAI values to the annual mean LAI values. The original and detrended 8 day LAI time series were used to drive the BEPS model, respectively.

2.4. Effects of greenness changes on ET and water yield

We conducted two model simulations on ET for China's terrestrial ecosystems over the period 2000–2014 using BEPS. The BEPS model was run at daily time step and was driven by meteorological data (temperature, precipitation, incoming solar radiation, and relative humidity), land cover type, atmospheric CO_2 concentrations, and soil properties data as described above. The original and detrended 8 day LAI time series were used to prescribe LAI for each pixel for the two simulations, and all other driving factors were exactly the same for these simulations.

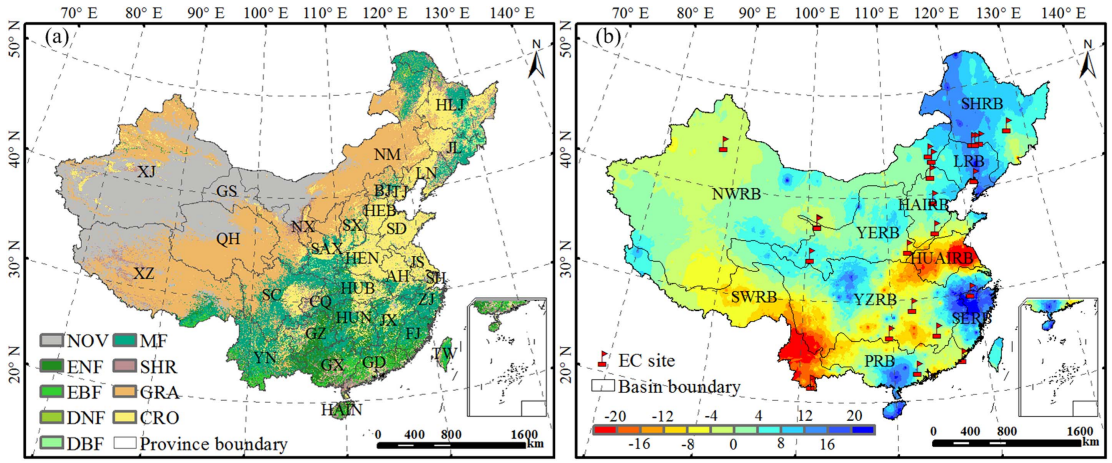

Figure 1. Depiction of the boundaries of provinces and large river basins over China and the distribution of EC flux sites used for the validation of simulated ET: (a) province boundaries; (b) river basin boundaries and distribution of EC sites. The base maps are the reclassified MODIS land cover map for (a) and the trends of annual precipitation (mm yr^{-1}) during the period 2000–2014 for (b), respectively. The land cover types are as follows: evergreen needleleaf forests (ENF), evergreen broadleaf forests (EBF), deciduous needleleaf forests (DNF), deciduous broadleaf forests (DBF), mixed forests (MF), shrublands (SHR), grasslands (GRA), croplands (CRO), and non-vegetation (NOV). The provinces, autonomous regions, or municipalities included in this study are as follows: Heilongjiang (HLJ), Neimenggu (NM), Xinjiang (XJ), Jilin (JL), Liaoning (LN), Gansu (GS), Hebei (HEB), Beijing (BJ), Shanxi (SX), Tianjin (TJ), Shaanxi (SAX), Ningxia (NX), Qinghai (QH), Shandong (SD), Xizang (XZ), Henan (HEN), Jiangsu (JS), Anhui (AH), Sichuan (SC), Hubei (HUB), Shanghai (SH), Zhejiang (ZJ), Hunan (HUN), Jiangxi (JX), Yunnan (YN), Guizhou (GZ), Fujian (FJ), Guangxi (GX), Guangdong (GD), Hainan (HAIN), and Taiwan (TW). The 10 river basins are as follows: Songhuajiang river basin (SHRB), Liaohe river basin (LRB), Haihe river basin (HAIRB), Yellow river basin (YERB), Huaihe river basin (HUAIRB), Yangtze river basin (YZRB), Southeast river basin (SERB), Pearl river basin (PRB), Southwest river basin (SWRB), and Northwest river basin (NWRB).

For each pixel, we calculated annual ET based on the simulated daily ET values for each simulation. Water yield (mm yr^{-1}) was estimated as follows:

$$WY = P - ET, \quad (4)$$

where WY, P, and ET are water yield, annual precipitation, and annual ET, respectively. This surface water balance approach assumes that the change in soil water and groundwater storage of catchment is negligible (Hare 1980, Sun *et al* 2006, Donohue *et al* 2007, Troy *et al* 2011). Many previous studies used this approach to estimate water yield at mesoscale or large scales (Sun *et al* 2005, Liu *et al* 2008a, Zhang *et al* 2009, Vinukollu *et al* 2011, Lu *et al* 2013).

The comparison of the two model simulations driven with original and detrended LAI allows us to assess how the changes in vegetation greenness affect the hydrological cycle. We compared the magnitude and spatial distribution of annual ET and water yield between the two simulations and then compared the trends of both annual ET and water yield. We assessed how the changes in vegetation greenness affected annual ET and water yield on a per-pixel basis and at the scale of large river basins (figure 1) so that we could determine how these effects varied with spatial scale.

3. Results

3.1. Trends and detrending of LAI

We examined the trends of vegetation greenness for China's terrestrial ecosystems using the annual mean LAI during the period from 2000 to 2014 (figure 2).

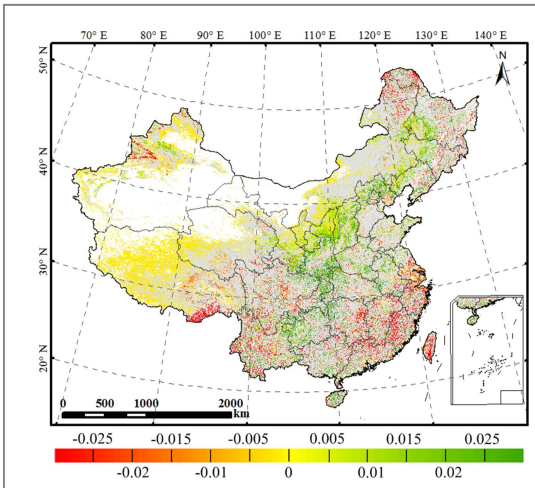

Figure 2. Trends of vegetation greenness as characterized by annual mean LAI for China's terrestrial ecosystems during the period 2000–2014. The units of the trends are m^2 m^{-2} yr^{-1}. The white color indicates non-vegetated areas, and light gray indicates vegetated areas with insignificant trends in annual mean LAI ($p > 0.05$).

Vegetation greenness as characterized by LAI exhibited statistically significant trends over 26.1% of China's land area; pixels with significant increasing and decreasing trends in LAI accounted for 15.8% and 10.3% of China's land area, respectively. Vegetation greening mainly occurred in central and northern China. LAI significantly increased by >=0.01 m^2 m^{-2} yr^{-1} in parts of Ningxia, Gansu, Shanxi, Shannxi, Hebei, Guizhou, Chongqing, Hunan, and Hubei. Vegetation browning was mainly observed in the

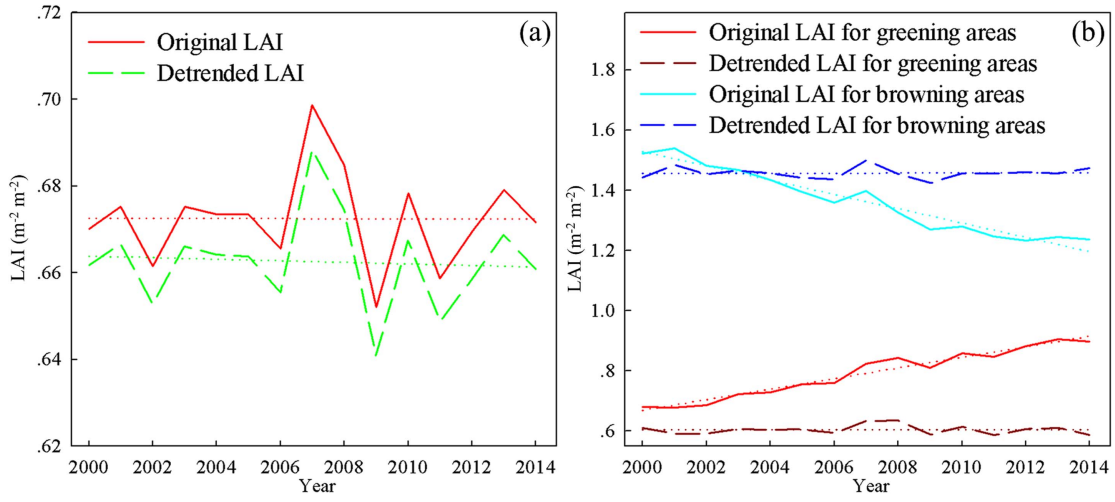

Figure 3. Spatially-averaged LAI over the period 2000–2014: (a) nationally-averaged original and detrended LAI; (b) original and detrended LAI for both greening and browning areas.

Southeast, Southwest, and Northeast. LAI decreased more than 0.02 m^2 m^{-2} yr^{-1} in southeastern coastal provinces (e.g., Jiangsu, Zhejiang, and Fujian) and in southern Tibet (0.03 m^2 m^{-2} yr^{-1}). Vegetation in Jiangxi, eastern Hunan, and parts of the Northeast also exhibited significant decreases in LAI. The nationally-averaged LAI time series did not exhibit a significant trend during the period 2000–2014 (figure 3(a)) likely because the increases in LAI were offset by the decreases elsewhere.

We detrended LAI for each pixel, and the significant increasing or decreasing trend was removed. The detrending of the LAI time series removed the increasing trends in LAI in areas with greening trends and also removed the decreasing trends in LAI in areas with browning trends (figure 3(b)). The mean LAI value of the browning areas was about 1.0 m^2 m^{-2} higher than that of the greening areas. This is likely because vegetation browning mainly occurred in more productive southern regions that had higher LAI than less productive northern regions with greening trends. The nationally-averaged detrended LAI retained the interannual variations of the nationally-averaged original LAI (figure 3(a)).

3.2. Evaluation of simulated annual ET and water yield

The ability of the BEPS model to simulate carbon and water fluxes of China's terrestrial ecosystems has been thoroughly evaluated against different sources of data (Liu *et al* 2015b). Here, we collected measured ET from 26 EC flux sites and runoff data from the 10 large river basins (figure 1) to evaluate the performance of BEPS in simulating ET and water yield, respectively. The 26 EC sites include 9 forest sites, 3 cropland sites, 12 grassland sites, and 2 wetland sites (Liu *et al* 2015b). The comparison between the simulated ET and the measured ET showed that BEPS estimated ET fairly well across sites (figure 4(a); $y = 0.79x + 91.2$, $R^2 = 0.77, p < 0.0001$).

We obtained annual runoff data for the 10 river basins over the period from 2000 to 2014 from the statistical data of 'China Water Resources Bulletin' (The Ministry of Water Resources of the People's Republic of China, http://mwr.gov.cn/zwzc/hygb/szygb/). According to the basin depiction on the hydrological yearbook of China, the mainland of China is divided into 10 major river basins: Songhua river basin (SHRB), Liaohe river basin (LRB), Haihe river basin (HAIRB), Yellow river basin (YERB), Huaihe river basin (HUAIRB), Yangtze river basin (YZRB), Southeast river basin (SERB), Pearl river basin (PRB), Southwest river basin (SWRB), and Northwest river basin (NWRB) (figure 1). The runoff data were converted to water yield with the units of mm yr^{-1} (referred to as measured water yield) based on the area of each basin. The simulated water yield showed excellent agreement with the measured water yield across river basins (figure 4(b); $y = 0.81x + 58.7$, $R^2 = 0.81$, $p < 0.0005$). We also compared the simulated and measured water yield over the period from 2000 to 2014 for each river basin separately (figure S5). The model estimated water yield fairly well over time for most of the river basins with R^2 value greater than 0.55 for most river basins. Water yield was overestimated for basins that croplands are widely distributed such as LRB, HAIRB, YERB, and HUAIRB likely because irrigation was not considered in the model and as a result ET was underestimated for croplands in these basins. Water yield was underestimated for NWRB likely because of the errors in precipitation interpolation resulting from the complex terrain.

We also compared our simulated ET against the MODIS ET product (Mu *et al* 2011) and EC-MOD ET (Xiao *et al* 2008, 2014). The EC-MOD dataset was developed from FLUXNET observations, MODIS data

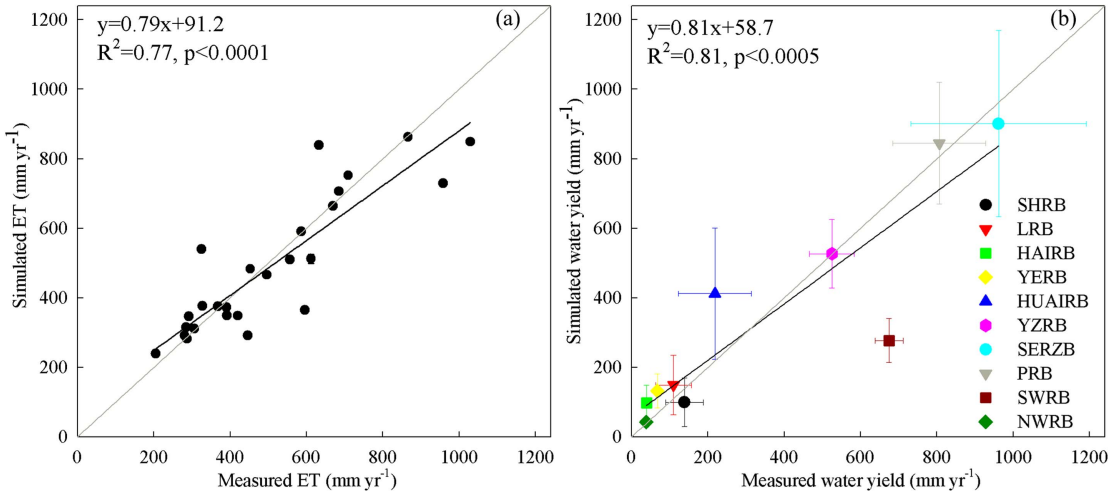

Figure 4. Evaluation of simulated annual ET and water yield: (a) simulated ET versus measured ET across the 26 EC sites; (b) simulated water yield versus measured water yield across the 10 river basins.

streams, and micrometeorological reanalysis data using a data-driven upscaling approach (Xiao *et al* 2008). The magnitude and spatial patterns of simulated ET were generally consistent with those of MODIS and EC-MOD ET (figure S6). The discrepancies between simulated and MODIS ET mainly occurred in southern regions of China. Simulated ET exhibited strong linear relationships with MODIS ET ($y = 1.01x + 96.8$, $R^2 = 0.64$, $p < 0.0001$) and EC-MOD ET ($y = 0.76x + 199.7$, $R^2 = 0.58$, $p < 0.0001$) on a per-pixel basis (figure S7). MODIS ET exhibited higher values than simulated ET. Our lower ET compared to MODIS ET was supported by EC flux tower measurements. A recent validation effort showed overestimation of MODIS ET for eight EC sites across China (Liu *et al* 2014c).

3.3. Spatial patterns of annual ET and water yield

We used the original and detrended LAI data to prescribe LAI, respectively, in BEPS model simulations and then examined how the changes in vegetation greenness affected the magnitude and spatial patterns of annual ET and water yield in China on a per-pixel basis (figure 5). Vegetation greening generally increased annual ET (figures 5(a) and (c)). Large differences in annual ET (~16%–20%) between the two simulations (original–detrended) were observed in regions with significant greening trends including parts of YERB. Northern HAIRB, LRB, and southern SHRB also showed large differences in annual ET (~12%–16%). The increase in annual ET by vegetation greening was ~5% in central YZRB and parts of HUAIRB. By contrast, vegetation browning generally decreased annual ET. Negative differences in annual ET between the two simulations (original–detrended) were sporadically distributed. Large decreases in ET (12%–16%) were observed in lower YZRB, northern SERB, and adjacent areas of upper YZRB and SWRB.

Changes in vegetation greenness also had significant effects on water yield on a per-pixel basis (figures 5(b) and (d)). Vegetation greening significantly decreased water yield, and large relative decreases in water yield (~16%–20%) between the two simulations (original–detrended) were observed in the regions with significant increasing trends in LAI, such as YERB, northern HAIRB, LRB, and southern SHRB. By contrast, vegetation browning led to increases in water yield. Large increases of water yield (~12%) were observed in the regions with decreasing ET. The spatial patterns of the changes in water yield between the two simulations were generally similar to those of the changes in annual ET but with the opposite direction and slightly larger magnitude (figure 5(d)).

3.4. Trends in annual ET and water yield

We assessed the trends of annual ET and water yield during the period 2000–2014 using the two model simulations prescribed with original LAI and detrended LAI, respectively (figure 6). Annual ET generally increased in regions with greening trends and decreased in regions with browning trends (figure 6(a)). Large positive trends in annual ET were observed in southeastern parts of LRB and eastern parts of YERB (8–12 mm yr^{-1}); moderate increases in annual ET (6–8 mm yr^{-1}) were sporadically distributed in southern river basins; small increases (2–4 mm yr^{-1}) were observed in central YERB. Compared with the simulated ET with original LAI, the simulated ET with detrended LAI exhibited weaker increasing trends in annual ET in many regions with greening trends and decreasing trends in annual ET in some regions with greening trends (figure 6(b)). The simulated ET with detrended LAI still increased in some regions mainly because of the increases in annual precipitation (figure 1(b)). Annual ET exhibited decreasing trends (>8 mm yr^{-1}) in regions of southern SWRB and lower YZRB with vegetation

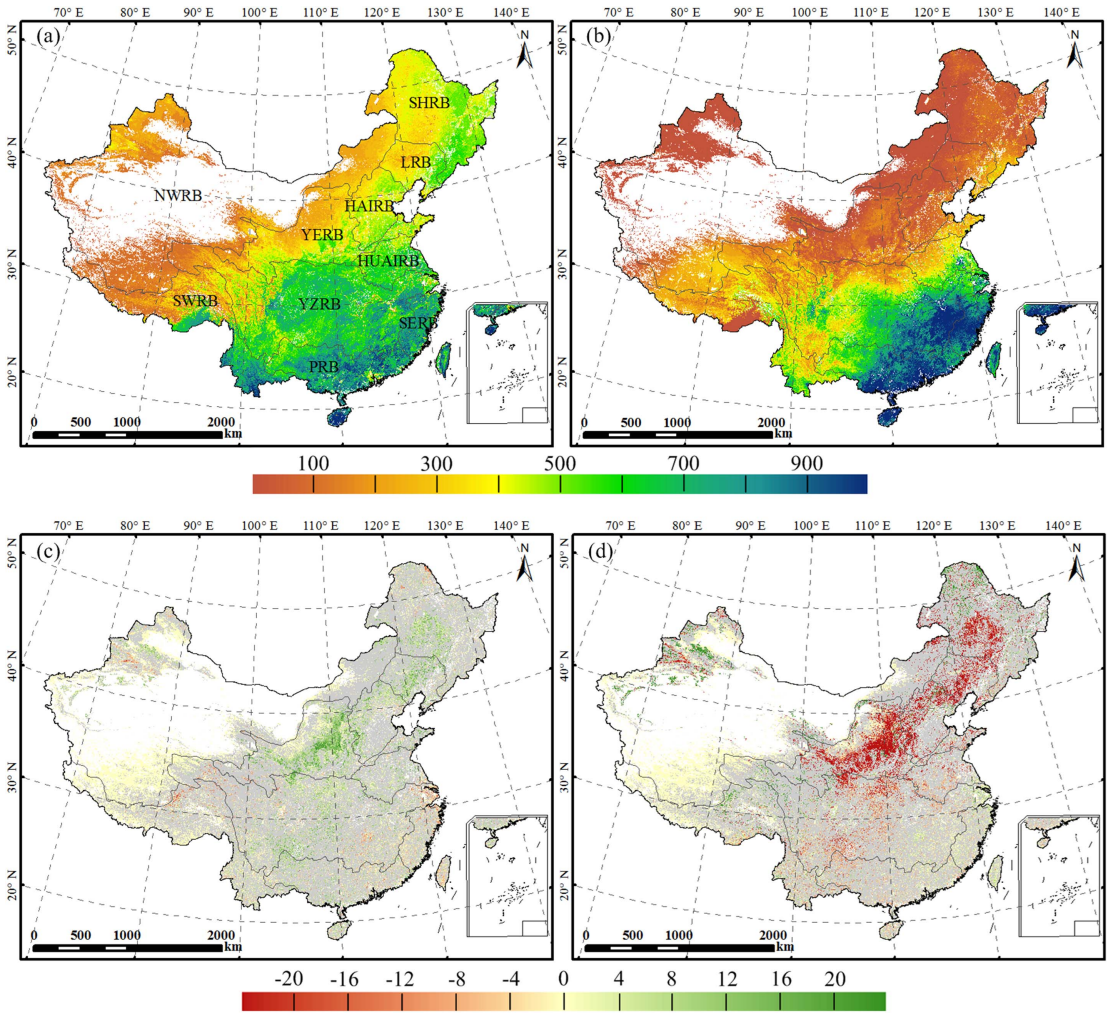

Figure 5. Magnitude and spatial distribution of mean annual ET and water yield in China over the period 2000–2014: (a) mean annual ET (mm yr^{-1}) and (b) mean annual water yield (mm yr^{-1}) simulated with original LAI; (c) the relative differences (%) in annual ET between the two model simulations (original–detrended); and (d) the relative differences (%) in water yield between the two model simulations (original–detrended).

browning and smaller decreasing trends (4–6 mm yr^{-1}) in other areas with decreasing LAI. The detrending of the LAI weakened the decreasing trends in annual ET in some regions with vegetation browning trends.

Modeled water yield with original LAI decreased in some areas with greening trends (figure 6(c)). In many other areas with greening trends (e.g., southern SHRB, eastern LRB, southern PRB, upper YZRB, and SERB), however, water yield increased (8–16 mm yr^{-1}) (figure 6(c)) because of the large increases in annual precipitation (figure 1(b)); the detrending of LAI led to larger increases in water yield in these regions (figure 6(d)). Our results showed that the greening trends slowed down the increases of water yield under the changing climate. For both simulations, water yield showed large decreases in HUAIRB and southern SWRB (~−20 mm yr^{-1}), moderate decreases (~−12 mm yr^{-1}) in central parts of YZRB, and small decreases in NWRB (−4 to −8 mm yr^{-1}) because of the moderate to large decreases in annual precipitation in these regions (figure 1(b)).

3.5. Effects of greenness trends on ET and water yield at national and large river basin scales

Nationally-averaged annual ET simulated with original LAI exhibited an upward trend over the 15 year period that was not statistically significant ($p = 0.12$) (figure 7(a)). With detrended LAI, the simulated annual ET also showed an insignificant upward trend ($p = 0.16$). The difference in nationally-averaged annual ET between the two simulations, however, exhibited a significant increasing trend ($y = 0.12x + 2.01$, $R^2 = 0.88$, $p < 0.0001$), indicating that vegetation greening increased nationally-averaged ET. Nationally-averaged water yield exhibited no significant trend over the 15 year period for the both simulations (figure 7(b)). The difference in nationally-averaged water yield between the two simulations, however, showed a decreasing trend ($y = -0.12x - 2.01$, $R^2 = 0.88$, $p < 0.0001$). Our results indicated that the changes in vegetation greenness slightly increased annual ET and decreased water yield at the national scale.

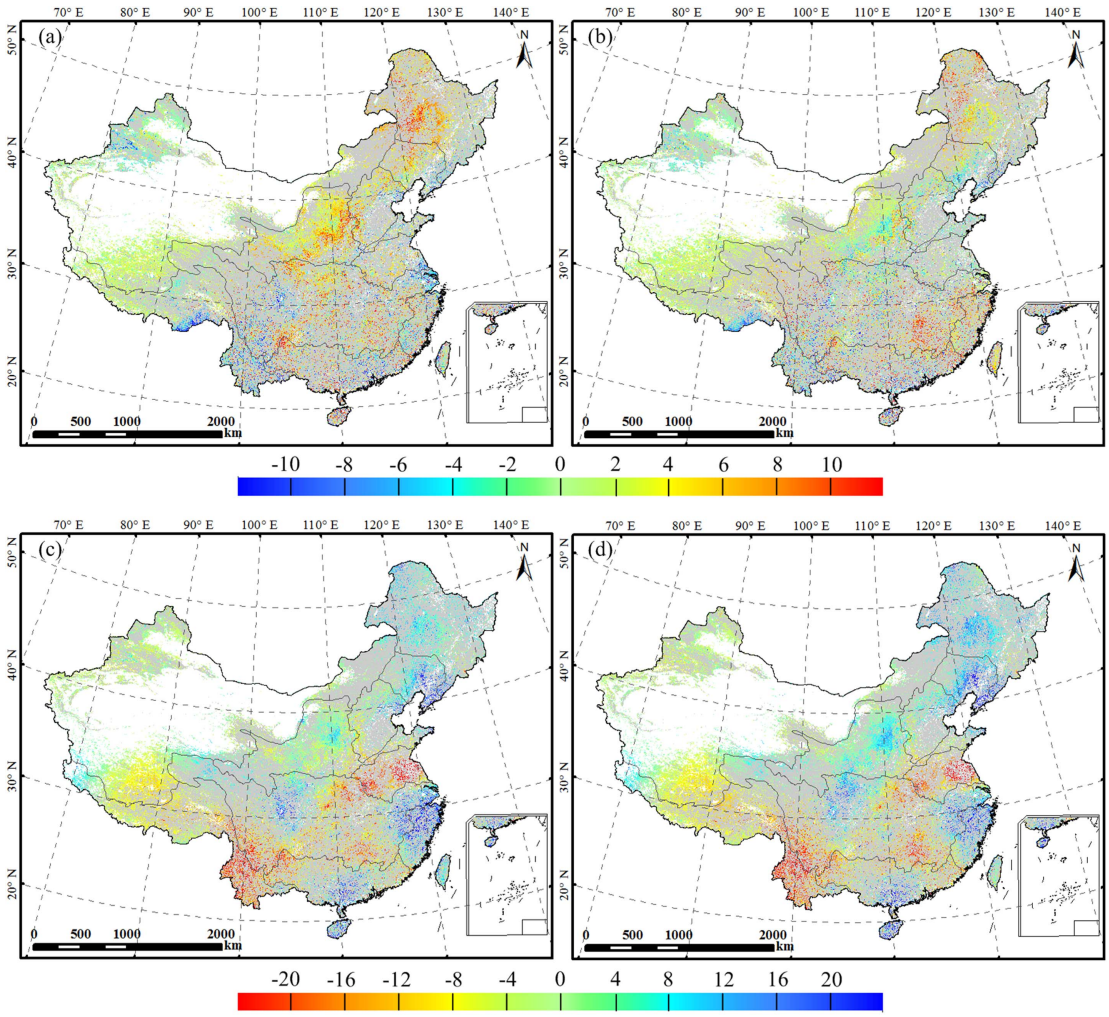

Figure 6. Trends of annual ET and water yield in China over the period 2000–2014: (a) simulated annual ET with original LAI; (b) simulated annual ET with detrended LAI; (c) simulated water yield with original LAI; and (d) simulated water yield with detrended LAI. The units are mm yr^{-1}.

We further examined how the trends in vegetation greenness affected annual ET and water yield for the 10 large river basins (figure 8). The annual mean LAI averaged at the large river basin scale significantly increased for LRB (0.004 m^2 m^{-2} yr^{-1}, $p < 0.05$), YERB (0.004 m^2 m^{-2} yr^{-1}, $p < 0.01$), and HAIRB (0.006 m^2 m^{-2} yr^{-1}, $p < 0.01$), and significantly decreased for SERB (−0.01 m^2 m^{-2} yr^{-1}, $p < 0.01$) and SWRB (−0.004 m^2 m^{-2} yr^{-1}, $p < 0.001$). The temporal trends of LAI were not significant for other 5 basins (HUAIRB, SHRB, YZRB, PRB, and NWRB).

The annual ET averaged over the river basin from both simulations significantly increased in SHRB (3.1 mm yr^{-1}, $p < 0.01$) and YERB (2.0 mm yr^{-1}, $p < 0.05$). The difference in annual ET between the two simulations exhibited significant increasing trends for SHRB (0.45 mm yr^{-1}, $R^2 = 0.88$, $p < 0.0001$), LRB (0.76 mm yr^{-1}, $R^2 = 0.94$, $p < 0.0001$), HAIRB (0.57 mm yr^{-1}, $R^2 = 0.95$, $p < 0.0001$), YERB (0.99 mm yr^{-1}, $R^2 = 0.98$, $p < 0.0001$), and HUAIRB (0.25 mm yr^{-1}, $R^2 = 0.84$, $p < 0.001$), significant decreasing trends for SERB (−1.07 mm yr^{-1}, $R^2 = 0.97$, p < 0.0001) and SWRB (−0.27 mm yr^{-1}, $R^2 = 0.93$, $p < 0.0001$), and no significant trends for YZRB ($p = 0.97$), PRB ($p = 0.38$), and NWRB ($p = 0.66$). These results showed that at the scale of large river basins, the greening trends could lead to increases in annual ET and the browning trends could reduce annual ET.

The changes in vegetation greenness also influenced water yield at the scale of large river basins (figure 9). The difference in water yield between the simulations with original and detrended LAI exhibited decreasing trends in SHRB (−0.45 mm yr^{-1}, $p < 0.0001$), LRB (−0.76 mm yr^{-1}, $p < 0.0001$), HAIRB (−0.57 mm yr^{-1}, $p < 0.0001$), and YERB (−0.99 mm yr^{-1}, $p < 0.0001$) that showed increasing trends in the difference of annual ET, increasing trends in HUAIRB (0.25 mm yr^{-1}, $p < 0.001$), SERB (1.07 mm yr^{-1}, $p < 0.0001$), and SWRB (0.27 mm yr^{-1}, $p < 0.0001$) that mostly showed decreasing trends in the difference of annual ET, and no significant trends in YZRB ($p = 0.97$), PRB ($p = 0.38$), and NWRB ($p = 0.66$) that showed no significant

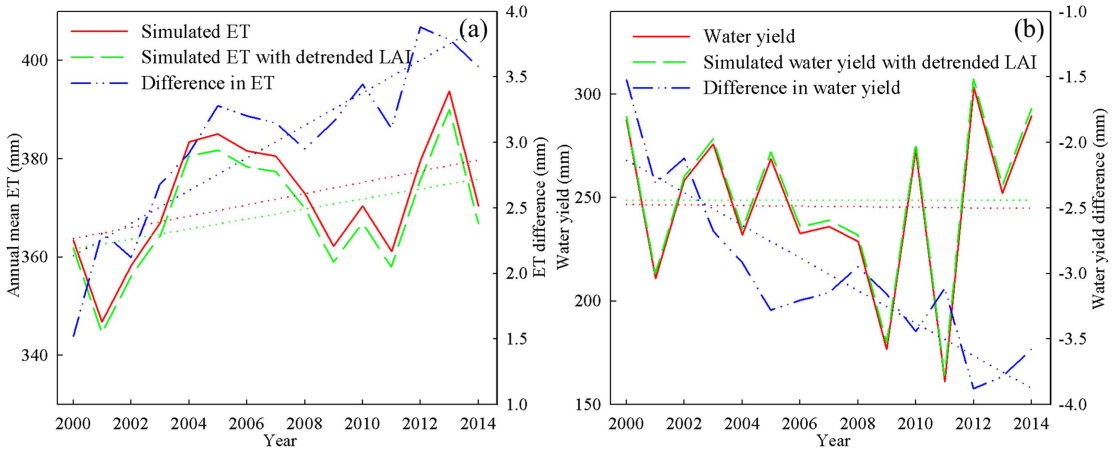

Figure 7. Trends of nationally-averaged annual ET (a) and water yield (b) during the period 2000–2014. The difference in ET (or water yield) stands for the difference in the simulated ET (or water yield) with original LAI and the simulated ET (or water yield) with detrended LAI.

trends in the difference in annual ET. The multi-year mean water yield over the period 2000–2014 between the two simulations exhibited largest differences for YERB, HAIRB, and LRB (~7%), intermediate differences for NWRB, SHRB (~3%) and HUAIRB (~1.5%), and smallest differences for YZRB, PRB, SERB (~0.5%), and SWRB (~0.1%). These results showed that the changes in vegetation greenness altered water yield at the scale of large river basins.

4. Discussion

Many studies have shown that vegetation greenness has been increasing over the last three decades based on long-term NDVI and/or LAI records (Xiao and Moody 2004, Park and Sohn 2010, Li *et al* 2012, Chen *et al* 2014, Xiao 2014). Changes in vegetation greenness in China were driven by multiple environmental and human factors (Tian *et al* 2011, Xiao *et al* 2015). Air temperature was the leading climatic factor driving the increases in vegetation productivity (Zhou *et al* 2001, Xiao *et al* 2015). Increasing precipitation also enhanced vegetation productivity in semi-arid and arid regions (Xiao *et al* 2015). The increase in diffuse radiation (Ren *et al* 2013) can also enhance plant growth (Xiao *et al* 2015). A modeling study indicated that rising atmospheric CO_2 significantly increased China's terrestrial carbon storage (Tian *et al* 2011). Nitrogen deposition enhanced vegetation productivity in regions with large increases in nitrogen deposition (Tian *et al* 2011, Xiao *et al* 2015). Forest plantations were partly responsible for the increases in vegetation greenness (Lu *et al* 2012, Xiao *et al* 2015, Zhang *et al* 2015b). Elevated crop yield resulting from improved agricultural management practices (e.g., improved irrigation infrastructure, increasing use of chemical fertilizers, and substitution of higher-yield crops for lower-yield crops) contributed to the increases in vegetation greenness (Xiao *et al* 2015). The relative contributions of these environmental and human factors to increasing vegetation greenness varied with spatial scale (Xiao *et al* 2015).

Despite the overall greening trends, browning trends were also observed in many areas in China. Multiple mechanisms are possibly responsible for the decreasing trends in vegetation greenness. The decline in vegetation greenness was mainly caused by ecosystem degradation (Li *et al* 2012) and urbanization (Liu and Gong 2012). Decreasing vegetation greenness in southeastern China and parts of southwestern China was possibly caused by the climatic abnormality (droughts and ice storm) and land cover changes (i.e., urbanization) (Peng *et al* 2011, Liu and Gong 2012, Liu *et al* 2012b). Vegetation browning in northeastern China was mainly associated with negative effects of increasing droughts (Peng *et al* 2011, Liu *et al* 2013a, 2014b). The vegetation greening and browning trends observed were generally consistent with those identified in previous studies (Chen *et al* 2014, Xiao 2014).

Our model simulations showed that on per-pixel basis, the increasing trends in LAI (vegetation greening) generally increased annual ET and decreased water yield, while decreasing trends in LAI (vegetation browning) decreased annual ET and increased water yield. The differences in annual ET and water yield between the two simulations exhibited increasing and decreasing trends, respectively, at the scales of large river basins and at the national scale, indicating that vegetation greening had positive effects on ET and negative effects on water yield at these spatial scales. Despite the effects of vegetation greening, the nationally-averaged annual ET and water yield did not exhibit significant increasing or decreasing trends. This is partly because vegetation greening trends only accounted for 15.8% of China's land area. For regions without significant changes in LAI or vegetation type,

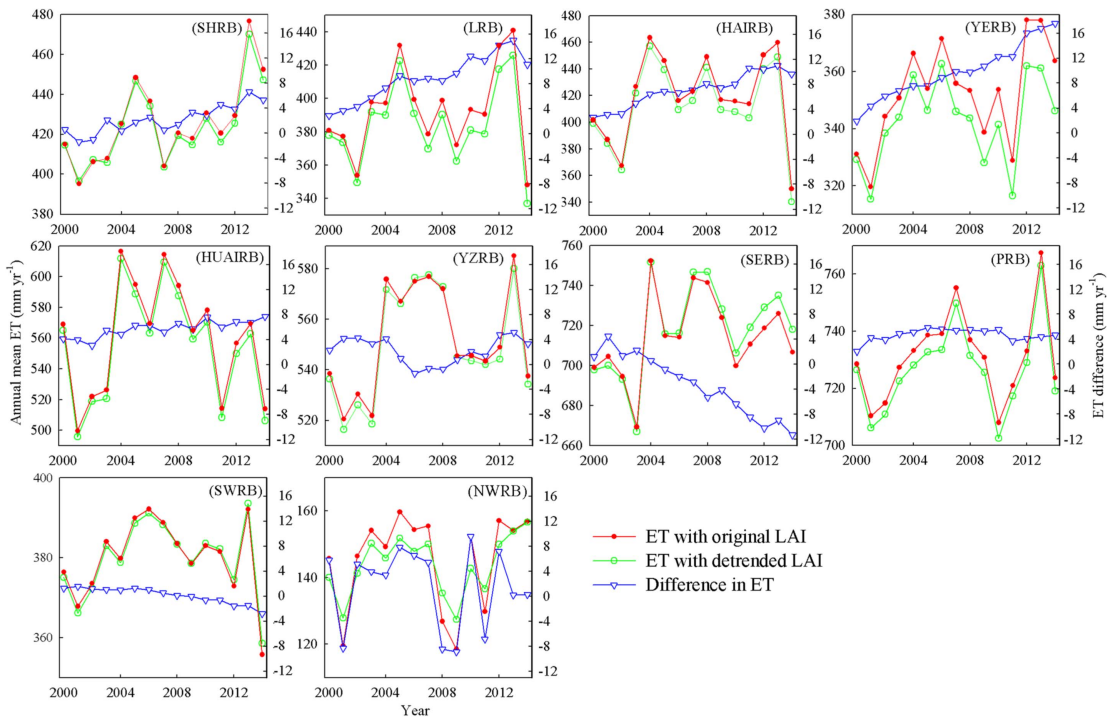

Figure 8. Spatially-averaged annual ET for the 10 river basins during the period 2000–2014. The difference in ET stands for the difference between the simulated ET with original LAI and the simulated ET with detrended LAI.

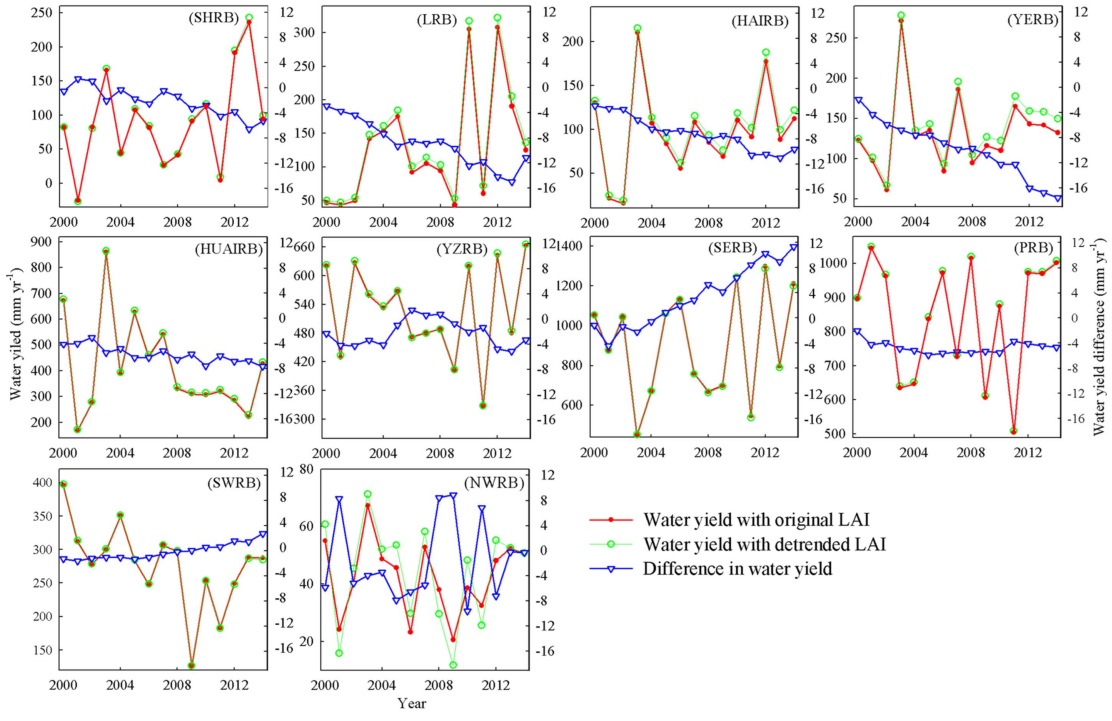

Figure 9. Spatially-averaged water yield for the 10 river basins during the period 2000–2014. The difference in water yield stands for the difference between the simulated water yield with original LAI and the simulated water yield with detrended LAI.

the changes in ET or water yield may follow different directions or exhibit no trends depending on the changes in precipitation and temperature. Moreover, vegetation browning was also observed in some regions, and the resulting decrease in ET and increase in water yield could partly offset the effects of vegetation greening. This indicates that the net effects of vegetation greening such as afforestation and reforestation on the hydrological cycle depend on the spatial scale. The State Forestry Administration of China expected that

the continued ecosystem restoration program will increase national forest cover to 26% by 2050 (Lei 2005). Vegetation greening therefore will likely have larger impacts on the hydrological cycle.

The effects of vegetation greening particularly afforestation projects on water yield have received growing attention. Some studies indicated that afforestation/reforestation caused significant increase of ET and reduction of streamflow (McVicar *et al* 2007, Yu *et al* 2009, Mátyás and Sun 2014, Yao *et al* 2015). Forests typically have higher ET than other vegetation types, and the conversion of croplands, grasslands, and bare lands to forests can lead to higher ET. For example, a pervious study showed that vegetation restoration resulted in different reduction of average water yield in the semiarid Loess Plateau region (50%) and the tropical southern region (30%), respectively (Sun *et al* 2006). By contrast, another study showed that forest recovery at Guangdong Province did not cause significant water reduction (Zhou *et al* 2010). A recent global-scale synthesis study indicated that land cover changes can lead to greater hydrological responses in non-humid regions or in watersheds of low water retention capacity (Zhou *et al* 2015). Our results showed that vegetation greening including afforestation/reforestation enhanced annual ET and reduced water yield, and the effects of vegetation greening on ET and water yield could be offset by other factors at the large river basin and the national scales. Our results also showed the difference between simulated water yield with original LAI and simulated water yield with detrended LAI was larger in northern river basins than in southern river basins, which indicates that vegetation change plays a larger role in regulating the water cycle in semi-humid, semi-arid, or arid areas.

There has been a debate on the feasibility and effectiveness of afforestation/reforestation efforts in northern China (Sun *et al* 2006, Cao 2008, Ma *et al* 2013). On one hand, afforestation/reforestation has improved ecological environment and sequestered more carbon in ecosystems (Liu *et al* 2014a). On the other hand, afforestation/reforestation could increase regional ET and reduce water yield, thereby aggravating the water shortage issue in northern China. Some previous studies argued that the feasibility of afforestation was constrained by the water availability in China's arid and semi-arid regions (Cao 2008). The carbon gain of ecosystems is associated with the cost of water consumption. Our results showed that afforestation/reforestation increased annual ET and reduced water yield. Afforestation efforts perhaps should focus on southern China with larger water supply given the water crisis in northern China (Hao *et al* 2015a) and the negative effects of these efforts on water yield (Xiao *et al* 2013).

Afforestation/reforestation induced changes in vegetation greenness can have feedbacks to the climate by altering the hydrological and energy cycles (van Dijk and Keenan 2007, Trabucco *et al* 2008, Ellison *et al* 2012, Jiang *et al* 2015). A regional climate modeling study indicated that the northern China forest shelterbelt project was likely to improve overall hydroclimatic conditions by increasing precipitation, relative humidity, and soil moisture (Liu *et al* 2008b). Using reanalysis atmospheric perceptible water and satellite vegetation index data, Jiang and Liang (2013) found that improved vegetation greenness strengthened ET and increased summer atmospheric water vapor over Northern China, indicating that afforestation/reforestation may have positive effects on regional water resources availability. Our results showed that the effects of the changes in vegetation greenness on ET and water yield varied with spatial scale. Assessing the net effects of vegetation greening/browning on annual ET and water yield in China requires the consideration of various environmental and human factors on plant productivity, mapping of the exact location and type of forests annually, and incorporation of the feedbacks to the climate.

5. Conclusions

We examined how the recent trends in vegetation greenness affected annual ET and water yield of China's terrestrial ecosystems during the period from 2000 to 2014. Significant trends of vegetation greenness were identified over 26.1% of China's land area, with 15.8% for greening and 10.3% for browning areas. Vegetation greening mainly occurred in central and northern China, while browning was mainly observed in southeastern, southwestern, and northeastern China. On a per-pixel basis, greening increased annual ET and decreased water yield, while browning reduced annual ET and increased water yield. At the large river basin and national scales, vegetation greening trends had positive effects on annual ET and had negative effects on water yield. The effects of the changes in vegetation greenness on the hydrological cycle depend on the spatial extent of the region and the fraction of greening or browning area. Our results indicate that afforestation efforts perhaps should focus on southern China where precipitation is abundant given the water crisis in northern China and the negative effects of vegetation greening on water yield. Future studies on the effects of vegetation greening/browning on the hydrological cycle at large scales should account for the feedbacks of the changes in ET and other biophysical properties (e.g., albedo) to the climate.

Acknowledgments

This study was funded by the National Natural Science Foundation of China (Grant No. 41401218), Key Research and Development Programs for Global Change and Adaptation (Grant No. 2016YFA0600202), the US National Science

Foundation through the MacroSystems Biology Program (Grant No. 1065777), the National Aeronautics and Space Administration (NASA) through the Science of Terra and Aqua (Grant No. NNX14AI70G) and Carbon Cycle Science Program (Grant No. NNX14AJ18G), the Jiangsu Key Laboratory of Agricultural Meteorology Foundation (KYQ1401), and China Special Fund for Meteorological Research in the Public Interest (Major projects) (GYHY201506001-6). We obtained the MODIS reflectance and land cover data from NASA (http://ladsweb.nascom.nasa.gov), MODIS ET data from the Numerical Terra dynamic Simulation Group, University of Montana, (http://ntsg.umt.edu), EC-MOD ET from Global Ecology Group, University of New Hampshire (http://globalecology.unh.edu), meteorological data from China Meteorological Administration (http://cdc.cma.gov.cn), and soil data from Beijing Normal University, China (http://globalchange.bnu.edu.cn). The digital boundary of river basins in China was kindly provided by Qiu'an Zhu, Northwest A & F University. We thank the anonymous reviewers for their constructive comments on the manuscript.

References

Andréassian V 2004 Waters and forests: from historical controversy to scientific debate *J. Hydrol.* **291** 1–27

Bao Z, Zhang J, Wang G, Fu G, He R, Yan X, Jin J, Liu Y and Zhang A 2012 Attribution for decreasing streamflow of the haihe river basin, northern China: climate variability or human activities? *J. Hydrol.* **460** 117–29

Bonan G B 2008 Forests and climate change: forcings, feedbacks, and the climate benefits of forests *Science* **320** 1444–9

Brown A E, Zhang L, McMahon T A, Western A W and Vertessy R A 2005 A review of paired catchment studies for determining changes in water yield resulting from alterations in vegetation *J. Hydrol.* **310** 28–61

Cao S 2008 Why large-scale afforestation efforts in China have failed to solve the desertification problem *Environ. Sci. Technol.* **42** 1826–31

Chen B *et al* 2014 Changes in vegetation photosynthetic activity trends across the Asia–Pacific region over the last three decades *Remote Sens. Environ.* **144** 28–41

Chen J M, Chen X Y, Ju W M and Geng X Y 2005 Distributed hydrological model for mapping evapotranspiration using remote sensing inputs *J. Hydrol.* **305** 15–39

Chen J M, Liu J, Cihlar J and Goulden M L 1999 Daily canopy photosynthesis model through temporal and spatial scaling for remote sensing applications *Ecol. Model.* **124** 99–119

Chen Y, Wang K, Lin Y, Shi W, Song Y and He X 2015 Balancing green and grain trade *Nat. Geosci.* **8** 739–41

de Jong R, de Bruin S, de Wit A, Schaepman M E and Dent D L 2011 Analysis of monotonic greening and browning trends from global NDVI time-series *Remote Sens. Environ.* **115** 692–702

Deng F, Chen J M, Plummer S, Chen M Z and Pisek J 2006 Algorithm for global leaf area index retrieval using satellite imagery *IEEE Trans. Geosci. Remote* **44** 2219–29

Donohue R J, Roderick M L and McVicar T R 2007 On the importance of including vegetation dynamics in Budyko's hydrological model *Hydrol. Earth Syst. Sci.* **11** 983–95

Ellison D, N Futter M and Bishop K 2012 On the forest cover-water yield debate: from demand-to supply-side thinking *Glob. Change Biol.* **18** 806–20

Friedl M A, Sulla-Menashe D, Tan B, Schneider A, Ramankutty N, Sibley A and Huang X M 2010 MODIS Collection 5 global land cover: algorithm refinements and characterization of new datasets *Remote Sens. Environ.* **114** 168–82

Gao Y, Zhu X, Yu G, He N, Wang Q and Tian J 2014 Water use efficiency threshold for terrestrial ecosystem carbon sequestration in China under afforestation *Agric. Forest Meteorol.* **195–196** 32–7

Garrigues S *et al* 2008 Validation and intercomparison of global leaf area index products derived from remote sensing data *J. Geophys. Res.-Biogeosci.* **113** G02028

Guay K C, Beck P S A, Berner L T, Goetz S J, Baccini A and Buermann W 2014 Vegetation productivity patterns at high northern latitudes: a multi-sensor satellite data assessment *Glob. Change Biol.* **20** 3147–58

Hao L, Sun G, Liu Y and Qian H 2015a Integrated modeling of water supply and demand under management options and climate change scenarios in Chifeng city, China *JAWRA J. Am. Water Resour. Assoc.* **51** 655–71

Hao L *et al* 2015b Urbanization dramatically altered the water balances of a paddy field-dominated basin in southern China *Hydrol. Earth Syst. Sci.* **19** 3319–31

Hare F K 1980 Long-term annual surface heat and water balances over Canada and the United States South of 60 °N: reconciliation of precipitation, run-off and temperature fields *Atmos. Ocean* **18** 127–53

Huang M, Zhang L and Gallichand J 2003 Runoff responses to afforestation in a watershed of the Loess Plateau, China *Hydrol. Process.* **17** 2599–609

Jackson R B, Jobbagy E G, Avissar R, Roy S B, Barrett D J, Cook C W, Farley K A, le Maitre D C, McCarl B A and Murray B C 2005 Trading water for carbon with biological sequestration *Science* **310** 1944–7

Jiang B and Liang S 2013 Improved vegetation greenness increases summer atmospheric water vapor over Northern China *J. Geophys. Res.-Atmos.* **118** 8129–39

Jiang B, Liang S and Yuan W 2015 Observational evidence for impacts of vegetation change on local surface climate over northern China using the Granger causality test *J. Geophys. Res.-Biogeosci.* **120** 1–12

Ju W M, Chen J M, Black T A, Barr A G, Liu J and Chen B Z 2006 Modelling multi-year coupled carbon and water fluxes in a boreal aspen forest *Agric. Forest Meteorol.* **140** 136–51

Ju W M, Gao P, Wang J, Zhou Y L and Zhang X H 2010a Combining an ecological model with remote sensing and GIS techniques to monitor soil water content of croplands with a monsoon climate *Agric. Water Manage.* **97** 1221–31

Ju W M, Gao P, Zhou Y L, Chen J M, Chen S and Li X F 2010b Prediction of summer grain crop yield with a process-based ecosystem model and remote sensing data for the northern area of the Jiangsu Province, China *Int. J. Remote Sens.* **31** 1573–87

Keeling C D, Bacastow R B, Bainbridge A E, Ekdahl C A, Guenther P R, Waterman L S and Chin J F S 1976 Atmospheric carbon dioxide variations at Mauna Loa Observatory, Hawaii *Tellus* **28** 538–51

Lei J 2005 *Forest Resources of China* (Beijing: Chinese Forestry) pp 172–3

Li A, Wu J and Huang J 2012 Distinguishing between human-induced and climate-driven vegetation changes: a critical application of RESTREND in inner Mongolia *Landscape Ecol.* **27** 969–82

Li S, Xu M and Sun B 2014 Long-term hydrological response to reforestation in a large watershed in southeastern China *Hydrol. Process.* **28** 5573–82

Liu D, Chen Y, Cai W, Dong W, Xiao J, Chen J, Zhang H, Xia J and Yuan W 2014a The contribution of China's grain to green program to carbon sequestration *Landscape Ecol.* **29** 1675–88

Liu H *et al* 2013a Rapid warming accelerates tree growth decline in semi-arid forests of Inner Asia *Glob. Change Biol.* **19** 2500–10

Liu J, Chen J M and Cihlar J 2003 Mapping evapotranspiration based on remote sensing: an application to Canada's landmass *Water Resour. Res.* **39** 1189

Liu J, Chen J M, Cihlar J and Park W M 1997 A process-based boreal ecosystem productivity simulator using remote sensing inputs *Remote Sens. Environ.* **62** 158–75

Liu J Y, Zhang Q and Hu Y F 2012a Regional differences of China's urban expansion from late 20th to early 21st century based on remote sensing information *Chin. Geogr. Sci.* **22** 1–14

Liu M L, Tian H Q, Chen G S, Ren W, Zhang C and Liu J Y 2008a Effects of land-use and land-cover change on evapotranspiration and water yield in China during 1900–2000 *J. Am. Water Resour. Assoc.* **44** 1193–207

Liu S and Gong P 2012 Change of surface cover greenness in China between 2000 and 2010 *Chin. Sci. Bull.* **57** 2835–45

Liu W, Wei X, Liu S, Liu Y, Fan H, Zhang M, Yin J and Zhan M 2015a How do climate and forest changes affect long-term streamflow dynamics? A case study in the upper reach of poyang river basin *Ecohydrology* **8** 46–57

Liu Y *et al* 2013b Evapotranspiration and water yield over China's landmass from 2000 to 2010 *Hydrol. Earth Syst. Sci.* **17** 4957–80

Liu Y, Ju W, Chen J, Zhu G, Xing B, Zhu J and He M 2012b Spatial and temporal variations of forest LAI in China during 2000–2010 *Chin. Sci. Bull.* **57** 2846–56

Liu Y, Stanturf J and Lu H 2008b Modeling the potential of the northern china forest shelterbelt in improving hydroclimate conditions1 *JAWRA J. Am. Water Resour. Assoc.* **44** 1176–92

Liu Y, Xiao J, Ju W, Zhou Y, Wang S and Wu X 2015b Water use efficiency of China's terrestrial ecosystems and responses to drought *Sci. Rep.* **5** 13799

Liu Y, Zhou Y, Ju W, Wang S, Wu X, He M and Zhu G 2014b Impacts of droughts on carbon sequestration by China's terrestrial ecosystems from 2000 to 2011 *Biogeosciences* **11** 2583–99

Liu Z, Shao Q and Liu J 2014c The performances of MODIS-GPP and -ET products in China and their sensitivity to input data (FPAR/LAI) *Remote Sens.* **7** 135–52

Lu N, Sun G, Feng X and Fu B 2013 Water yield responses to climate change and variability across the North–South Transect of Eastern China (NSTEC) *J. Hydrol.* **481** 96–105

Lu Y, Fu B, Feng X, Zeng Y, Liu Y, Chang R, Sun G and Wu B 2012 A policy-driven large scale ecological restoration: quantifying ecosystem services changes in the Loess Plateau of China *PLoS One* **7** e31782

Ma H, Lv Y and Li H 2013 Complexity of ecological restoration in China *Ecol. Eng.* **52** 75–8

Makarieva A M, Gorshkov V G and Li B-L 2006 Conservation of water cycle on land via restoration of natural closed-canopy forests: implications for regional landscape planning *Ecol. Res.* **21** 897–906

McVicar T R *et al* 2007 Developing a decision support tool for China's re-vegetation program: simulating regional impacts of afforestation on average annual streamflow in the Loess Plateau *Forest Ecol. Manage.* **251** 65–81

Mu Q Z, Zhao M S and Running S W 2011 Improvements to a MODIS global terrestrial evapotranspiration algorithm *Remote Sens. Environ.* **115** 1781–800

Mátyás C and Sun G 2014 Forests in a water limited world under climate change *Environ. Res. Lett.* **9** 085001

Park H-S and Sohn B J 2010 Recent trends in changes of vegetation over East Asia coupled with temperature and rainfall variations *J. Geophys. Res.-Atmos.* **115** D14101

Peng S, Chen A, Xu L, Cao C, Fang J, Myneni R B, Pinzon J E, Tucker C J and Piao S 2011 Recent change of vegetation growth trend in China *Environ. Res. Lett.* **6** 044027

Pisek J, Chen J M and Deng F 2007 Assessment of a global leaf area index product from SPOT-4 VEGETATION data over selected sites in Canada *Can. J. Remote Sens.* **33** 341–56

Ren X L, He H L, Zhang L, Zhou L, Yu G R and Fan J W 2013 Spatiotemporal variability analysis of diffuse radiation in China during 1981–2010 *Ann. Geophys.* **31** 277–89

Shangguan W, Dai Y, Liu B, Ye A and Yuan H 2012 A soil particle-size distribution dataset for regional land and climate modelling in China *Geoderma* **171–172** 85–91

Sheil D and Murdiyarso D 2009 How forests attract rain: an examination of a new hypothesis *Bioscience* **59** 341–7

Sun G, McNulty S G, Lu J, Amatya D M, Liang Y and Kolka R K 2005 Regional annual water yield from forest lands and its response to potential deforestation across the southeastern United States *J. Hydrol.* **308** 258–68

Sun G, Zhou G Y, Zhang Z Q, Wei X H, McNulty S G and Vose J M 2006 Potential water yield reduction due to forestation across China *J. Hydrol.* **328** 548–58

Tian H Q *et al* 2011 China's terrestrial carbon balance: contributions from multiple global change factors *Glob. Biogeochem. Cycles* **25** GB1007

Trabucco A, Zomer R J, Bossio D A, van Straaten O and Verchot L V 2008 Climate change mitigation through afforestation/reforestation: a global analysis of hydrologic impacts with four case studies *Agric. Ecosyst. Environ.* **126** 81–97

Troy T J, Sheffield J and Wood E F 2011 Estimation of the terrestrial water budget over northern eurasia through the use of multiple data sources *J. Clim.* **24** 3272–93

van Dijk A and Keenan R J 2007 Planted forests and water in perspective *Forest Ecol. Manage.* **251** 1–9

Vermote E and Vermeulen A 1999 Atmospheric correction algorithm: spectral reflectances (MOD09), *ATBD version* 4

Vinukollu R K, Wood E F, Ferguson C R and Fisher J B 2011 Global estimates of evapotranspiration for climate studies using multi-sensor remote sensing data: evaluation of three process-based approaches *Remote Sens. Environ.* **115** 801–23

Wang G L and You L Z 2004 Delayed impact of the North Atlantic oscillation on biosphere productivity in Asia *Geophys. Res. Lett.* **31** L12210

Wang L *et al* 2012 China's urban expansion from 1990 to 2010 determined with satellite remote sensing *Chin. Sci. Bull.* **57** 2802–12

Xiao J and Moody A 2005 Geographical distribution of global greening trends and their climatic correlates: 1982–1998 *Int. J. Remote Sens.* **26** 2371–90

Xiao J *et al* 2013 Carbon fluxes, evapotranspiration, and water use efficiency of terrestrial ecosystems in China *Agric. Forest Meteorol.* **182–183** 76–90

Xiao J *et al* 2014 Data-driven diagnostics of terrestrial carbon dynamics over North America *Agric. Forest Meteorol.* **197** 142–57

Xiao J F 2014 Satellite evidence for significant biophysical consequences of the 'grain for green' program on the Loess Plateau in China *J. Geophys. Res.-Biogeosci.* **119** 2261–75

Xiao J F and Moody A 2004 Trends in vegetation activity and their climatic correlates: China 1982–1998 *Int. J. Remote Sens.* **25** 5669–89

Xiao J F, Zhou Y and Zhang L 2015 Contributions of natural and human factors to increases in vegetation productivity in China *Ecosphere* **6** 233

Xiao J F *et al* 2008 Estimation of net ecosystem carbon exchange for the conterminous United States by combining MODIS and AmeriFlux data *Agric. Forest Meteorol.* **148** 1827–47

Xie X, Liang S, Yao Y, Jia K, Meng S and Li J 2015 Detection and attribution of changes in hydrological cycle over the Three-North region of China: Climate change versus afforestation effect *Agric. Forest Meteorol.* **203** 74–87

Yao Y, Cai T, Ju C and He C 2015 Effect of reforestation on annual water yield in a large watershed in northeast China *J. Forestry Res.* **26** 697–702

Yu P, Krysanova V, Wang Y, Xiong W, Mo F, Shi Z, Liu H, Vetter T and Huang S 2009 Quantitative estimate of water yield reduction caused by forestation in a water-limited area in northwest China *Geophys. Res. Lett.* **36** L02406

Zhang F, Ju W, Shen S, Wang S, Yu G and Han S 2013 How recent climate change influences water use efficiency in East Asia *Theor. Appl. Climatol.* **116** 359–70

Zhang K, Kimball J S, Mu Q Z, Jones L A, Goetz S J and Running S W 2009 Satellite based analysis of northern ET trends and associated changes in the regional water balance from 1983 to 2005 *J. Hydrol.* **379** 92–110

Zhang K, Kimball J S, Nemani R R, Running S W, Hong Y, Gourley J J and Yu Z 2015a Vegetation greening and climate change promote multidecadal rises of global land evapotranspiration *Sci. Rep.* **5** 15956

Zhang L, Dawes W R and Walker G R 2001 Response of mean annual evapotranspiration to vegetation changes at catchment scale *Water Resour. Res.* **37** 701–8

Zhang Y *et al* 2015b Multiple afforestation programs accelerate the greenness in the 'Three North' region of China from 1982 to 2013 *Ecol. Indicators* **61** 404–12

Zhou G *et al* 2011 Quantifying the hydrological responses to climate change in an intact forested small watershed in Southern China *Glob. Change Biol.* **17** 3736–46

Zhou G *et al* 2015 Global pattern for the effect of climate and land cover on water yield *Nat. Commun.* **6** 5918

Zhou G Y, Wei X H, Luo Y, Zhang M F, Li Y L, Qiao Y N, Liu H G and Wang C L 2010 Forest recovery and river discharge at the regional scale of Guangdong Province, China *Water Resour. Res.* **46** W09503

Zhou L M, Tucker C J, Kaufmann R K, Slayback D, Shabanov N V and Myneni R B 2001 Variations in northern vegetation activity inferred from satellite data of vegetation index during 1981–1999 *J. Geophys. Res.-Atmos.* **106** 20069–83